SSC-MAG-55
LBL-20176

REVIEW OF TAC SUPERFERRIC MAGNET*

S. Marks, D. Humphries

Lawrence Berkeley Laboratory
University of California
Berkeley, California 94720

September 3, 1985

* This work was supported by the Director, Office of Energy Research, Office of High Energy and Nuclear Physics, High Energy Physics Division, U. S. Dept. of Energy, under Contract No. DE-AC03-76SF00098

REVIEW OF TAC SUPERFERRIC MAGNET

S. Marks, D. Humphries

Lawrence Berkeley Laboratory
University of California
Berkeley, California 94720

Introduction

This report reviews the technical investigation carried out by the authors on behalf of the SSC Central Design Group of the TAC superferric magnet design. The studies reported here include conductor current level optimizations at 0.15 T, 2.0 T, 3.0 T, and 3.25 T, maximum conductor fields at 3.25 T, sensitivity of field quality to variations in the magnetic shunt, and affects of up-down asymmetries.

The general features of the design are shown in Fig. 1, which is a diagram of the upper right-hand quadrant of the magnet cross-section. In particular, this design is characterized by a magnetic shunt which separates the aperture from the primary coils. The current in the three coils, labeled I_c, I_{in}, and I_{out}, may be individually controlled. Two configurations of the trim coil, labeled I_c, were investigated. The nominal location is indicated by the solid contour in Fig. 1; the alternate location, displaced vertically by -0.06",is indicated by the dashed contour. The three currents are to be used as parameters to control the dipole field value, and to zero the first two allowed harmonic components, the sextupole and decapole.

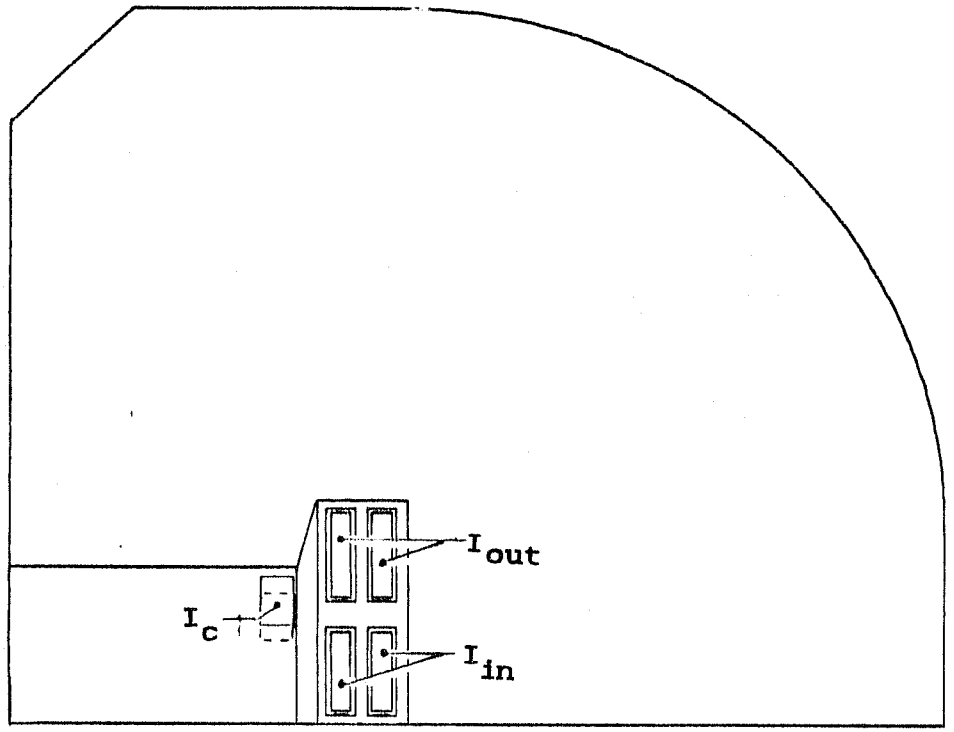

Fig 1, Upper Right Hand Quadrant

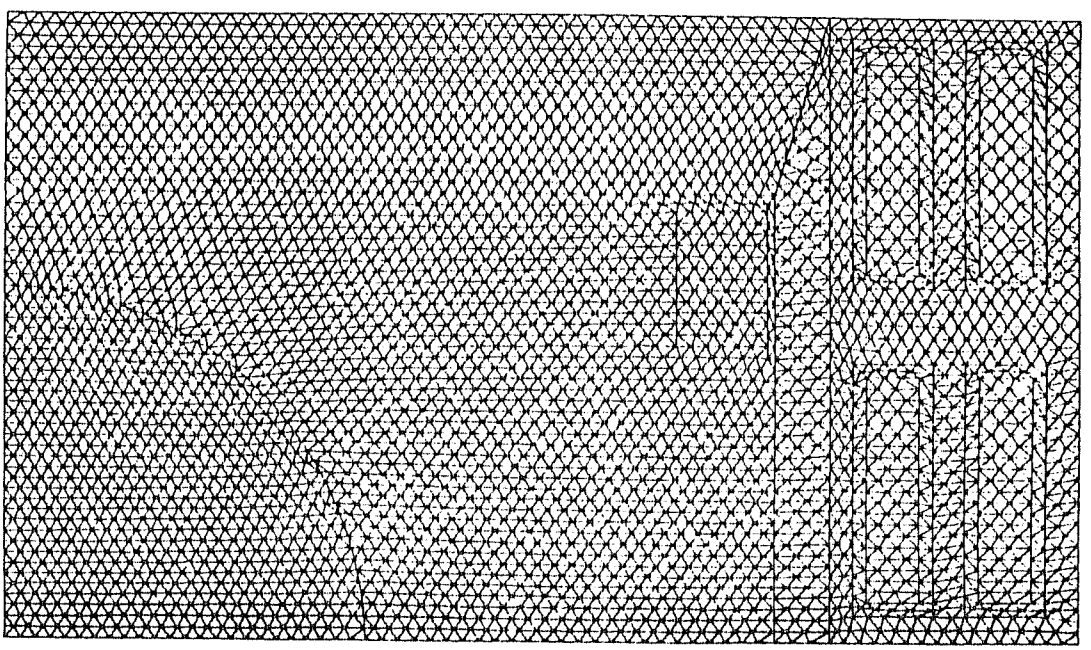

Fig 2, Mesh in Aperture and Coil Region

Magnet Model

The analysis reported here relied upon the use of the magnet modeling code POISSON, and its related optimization code MIRT. A great deal of care was taken to set up the model to insure accuracy in the calculations. The total number of node points was near the maximum allowed. Fig. 2 shows the mesh in the aperture, and coil region.

The integration arc used to compute the harmonic field coefficients is defined by 48 equally spaced points on a radius of 1.0 cm. The mesh was constructed such that the integration points correspond to mesh node points; this insures greatest accuracy for the calculation of the field at these points, since no interpolation is required at node points. The integration arc is apparent in the mesh of Fig. 2.

Part I - Current Optimization

Tables 1 through 4 report the results for 0.15 T, 2.0 T, 3.0 T, and 3.25 T field levels, respectively. For 2.0 T and 3.25 T results are included for the two different locations of the trim coil, labeled I_c in Fig. 1. The 0.15 T and 3.0 T cases include results only for the nominal location of the trim coil.

The notation for the harmonic coefficients relates to the following form for B^*:

$$B^* = B_x - iB_y = \Sigma\, c_n z^n \; ; \quad c_n = a_n + ib_n .$$

For the ideal symmetries represented by the quadrant model, the only allowed harmonics are b_0, b_2, b_4, etc. The coeficients b_n ($n \neq 0$) are normalized by b_0 and reported in units of 10^{-4}.

POISSON was used to obtain initial current values which correspond to the target value for b_0. This initial solution was then used as input to MIRT to search for a local minimum of the objective function. In each of the cases, the objective function was the sum of the squared values of b_2 and b_4. The free variables were two of the three currents; the third current, the largest of the three from the initial evaluation, was held fixed. In general, since the total current was not constrained, the fundamental, b_0, drifted slightly as a result of the optimization.

Table 1
0.15 T, Nominal Trim Coil Location

Currents (kA)			Harmonic Coefficients				
I_c	I_{out}	I_{in}	b_0(T)	$b_2(10^{-4})$	$b_4(10^{-4})$	$b_6(10^{-4})$	$b_8(10^{-4})$
0.146	0.024	0.658	0.149	-0.892	0.033	0.076	0.035

Table 2a
2.0 T, Nominal Trim Coil Location

Currents (kA)			Harmonic Coefficients				
I_c	I_{out}	I_{in}	b_0(T)	$b_2(10^{-4})$	$b_4(10^{-4})$	$b_6(10^{-4})$	$b_8(10^{-4})$
1.872	0.040	9.077	1.961	-2.213	2.722	1.534	0.448

The 2.0 T solution reported in Table 2a, with the nominal trim coil location, did not satisfy the criteria within MIRT for a local minimum. However, the convergence rate was so slow that MIRT terminated without finding a solution. A series of optimizations were attempted without improving on these results.

Table 2b
2.0 T, Alternate Trim Coil Location

Currents (kA)			Harmonic Coefficients				
I_c	I_{out}	I_{in}	b_0(T)	$b_2(10^{-4})$	$b_4(10^{-4})$	$b_6(10^{-4})$	$b_8(10^{-4})$
2.539	0.062	9.258	2.055	-0.517	2.382	0.378	0.161

Notice that the alternate trim coil location resulted in an improved solution, as shown in Table 2b. In this case the solution is a local minimum. Although the value of b_4 did not improve dramatically compared to case 2a, b_2 did drop below 1 unit; a side effect was an improved value for b_6.

Table 3
3.0 T, Nominal Trim Coil Location

Currents (kA)			Harmonic Coefficients				
I_c	I_{out}	I_{in}	b_0(T)	$b_2(10^{-4})$	$b_4(10^{-4})$	$b_6(10^{-4})$	$b_8(10^{-4})$
-2.644	9.957	11.302	2.944	0.052	-0.058	2.879	0.522

Notice that while the local minimum for this case corresponds to low values for b_2 and b_4, the value for b_6, which is not being controlled, is the dominant coefficient for this case.

Table 4a
3.25 T, Nominal Trim Coil Location

Currents (kA)			Harmonic Coefficients				
I_c	I_{out}	I_{in}	b_0(T)	$b_2(10^{-4})$	$b_4(10^{-4})$	$b_6(10^{-4})$	$b_8(10^{-4})$
-5.265	15.278	11.379	3.198	1.461	-0.558	3.238	0.585

Table 4b
3.25 T, Alternate Trim Coil Location

Currents (kA)			Harmonic Coefficients				
I_c	I_{out}	I_{in}	b_0(T)	$b_2(10^{-4})$	$b_4(10^{-4})$	$b_6(10^{-4})$	$b_8(10^{-4})$
-5.588	15.278	12.297	3.247	-1.040	-1.751	4.756	1.191

At 3.25 T, reasonable values for b_2 and b_4 were found for both coil configurations. However, the relative value of b_6 is quite large, particularly for the alternate trim coil location, reported in Table 4b. The results reported in Tables 4a and 4b together with those of Table 3 suggest that an additional control is required at fields of 3.0 T and above to maintain acceptable values for b_6.

Part II - Maximum Conductor Fields

The maximum field value was checked at 3.0 T and 3.25 T with and without the magnetic shunt. The results are illustrated in Figs. 3 and 4. The maximum field point is different for 3.0 T and 3.25 T. Also the value as a percentage of the central field, for the case with the shunt, has increased from 100% to 121%. In both cases the maximum field value is increased by removing the shunt. In all cases, the maximum field point lies on the edge of the conductor closest to the aperture. By refering to Tables 3 and 4, we also see that in each case the maximum field point occurs where the current is also the highest.

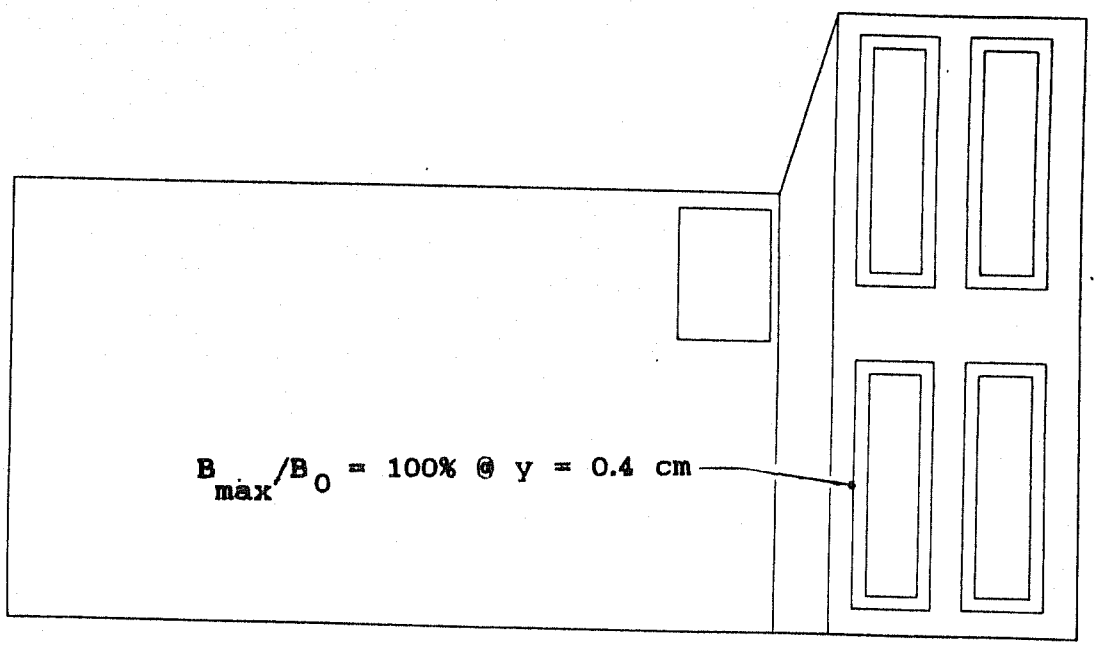

Fig 3a, B_0 = 2.94 T - With Shunt

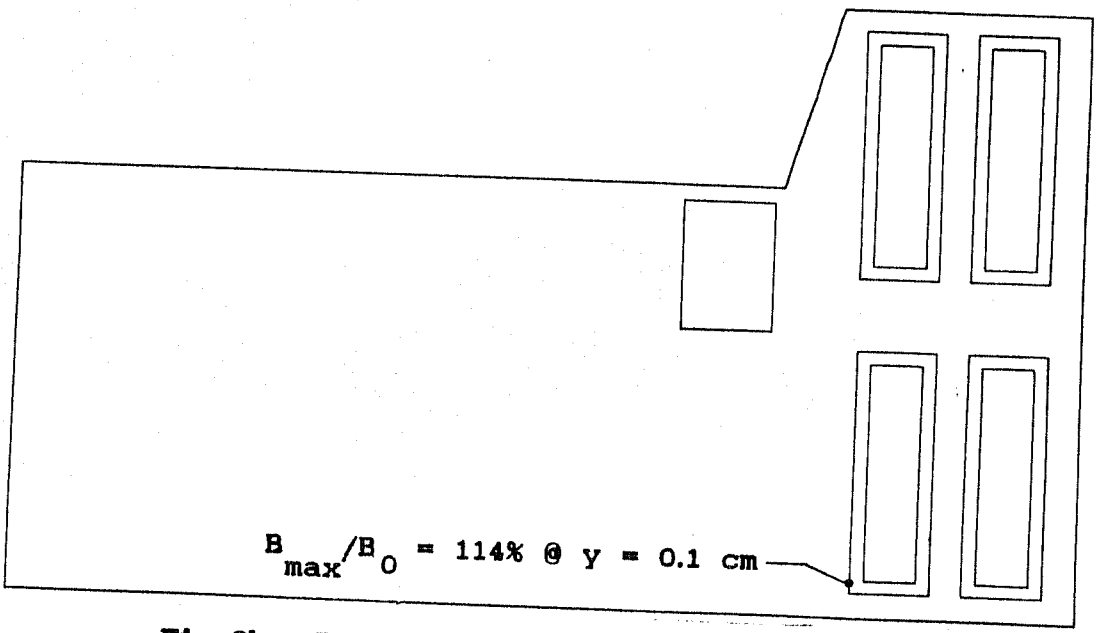

Fig 3b, B_0 = 2.98 T - Without Shunt

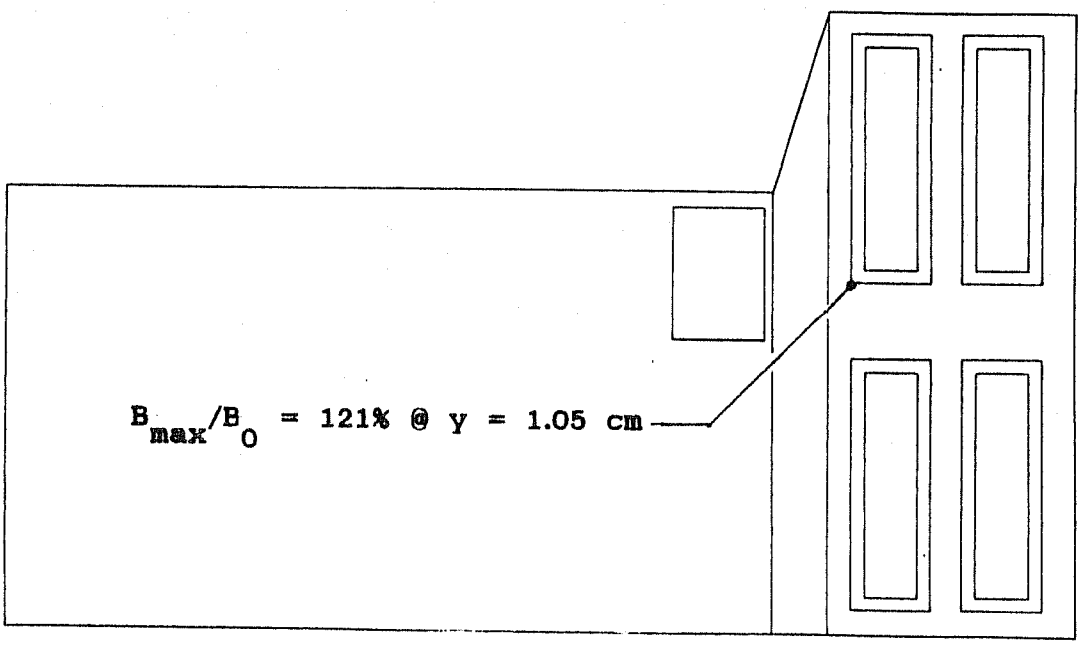

Fig 4a, B_0 = 3.29 T - With Shunt

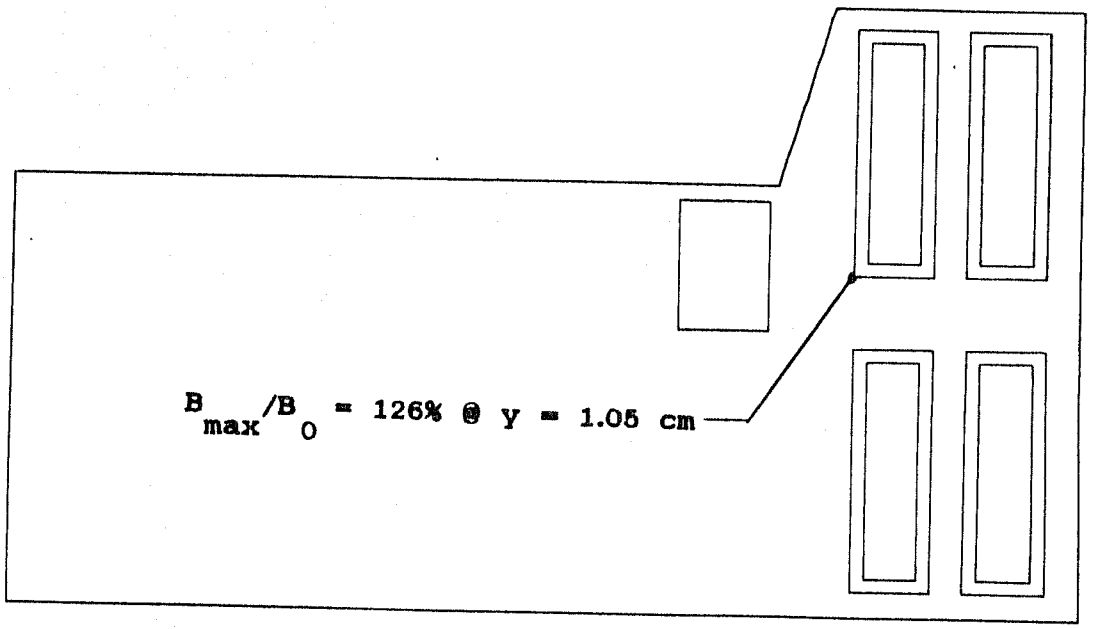

Fig 4b, B_0 = 3.29 T - Without Shunt

Part III - Field Sensitivity to Shunt Variations

The previous sections dealt with the characteristics of the ideal TAC magnet; ie., the characteristics which are expected to correspond to a magnet built exactly to specification. This section and the following section discuss the sensitivity of the field quality to deviations from the ideal magnet.

Variations in Magnetic Shunt Thickness

The infuence of the magnetic shunt on the field changes greatly over the range of central field values, from injection to maximum field. At a central field value of 0.15 T the value of the permeability, μ, in the shunt is about 15.0. This value is low compared to μ in the pole piece, but still large compared to 1.0, the value for vacuum. At a central field value of 3.25 T, μ has decreased to about 1.6.

Consider the 0.15 T case. Because μ is large compared to 1.0, the magnetic flux is constrained to be approximately constant through all horizontal cross-sections of the shunt. Scalar potential lines are constrained to be approximately perpendicular to the vertical boundaries of the shunt and with uniform spacing. However, for this case, since the value of μ is not so large as to be effectively infinite, the uniformity of scalar potential lines, and their associated field lines in the vicinity of the shunt is directly tied to the geometric and material uniformity of the shunt. In particular, local variations in either its thickness or its value of μ will directly affect the field uniformity.

This observation was tested by making small variations in the shunt thickness. The variation took the form of a notch of 0.0057 cm (2.85 mils) deep by 0.3 cm high; the notch was also tapered at each end, to reduce possible corner affects. The only field investigated here was 0.15 T since the affect is expected to be smaller for higher fields. Figs. 5a, 5b, and 5c show the shunt with a schematic illustration of the three different notch locations which were considered. Note that the notch depth is greatly exaggerated in the figures. The corresponding results are reported in the accompanying tables.

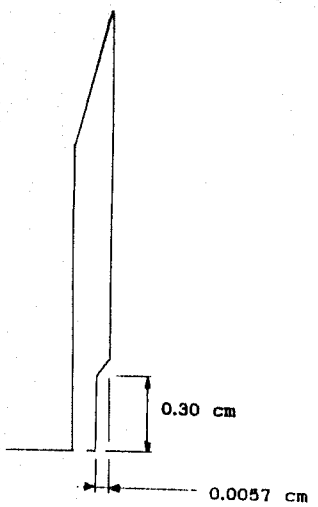

Fig. 5a

Table 5a

	b_n	Δb_n *
b_2:	11.067	10.174
b_4:	6.866	6.538
b_6:	2.457	1.695
b_8:	0.705	0.350
b_{10}:	0.357	0.070

* $\Delta \equiv |b_n| - |b_n'|$

b_n' are values in Table 1.

$B_0 = 0.149$ T

$I_c = 0.146$ kA, $I_{out} = 0.024$ kA, $I_{in} = 0.658$ kA

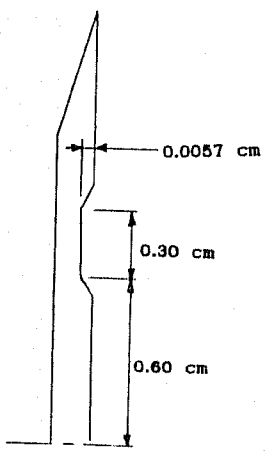

Fig. 5b

Table 5b

	b_n	Δb_n *
b_2:	−6.648	5.756
b_4:	−3.033	2.705
b_6:	−0.247	−0.516
b_8:	0.123	−0.232
b_{10}:	0.248	−0.040

* $\Delta \equiv |b_n| - |b_n'|$

b_n' are values in Table 1

$B_0 = 0.149$ T

$I_c = 0.146$ kA, $I_{out} = 0.024$ kA, $I_{in} = 0.658$ kA

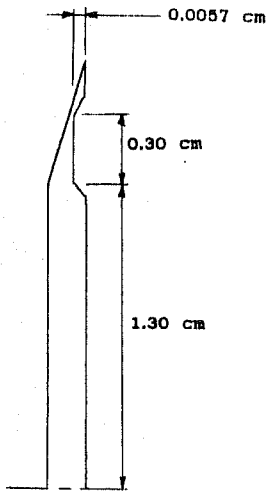

Fig. 5c

Table 5c

	b_n	Δb_n *
b_2:	-1.098	0.205
b_4:	2.350	-0.093
b_6:	0.752	-0.013
b_8:	0.360	0.005
b_{10}:	0.287	-0.001

* $\Delta = |b_n| - |b_n'|$
b_n' are values in Table 1

$B_0 = 0.149$ T

$I_c = 0.146$ kA, $I_{out} = 0.024$ kA, $I_{in} = 0.658$ kA

All of the shunt nonuniformities considered above correspond to variations within the normal quadrant symmetry (the next section considers asymmetric variations). Although nonuniformities due to manufacturing are not in general expected to correspond to these symmetries, these results indicate an extreme sensitivity in field quality to shunt nonuniformities. In particular, as indicated in Table 5a, sensitivity is very high for nonuniformities near the horizontal midplane. Variations in shunt thickness of several 0.001 cm are very likely. Variations of several percent in local value of μ is expected to cause similar results.

Other Affects of the Magnetic Shunt

In addition to the numerical results discussed above, there are several significant qualitative observations which will be discussed here. Refer to Figs. 6, 7, and 8, which show field line plots for 0.15 T, 2.0 T, and 3.25 T fields, respectively. In particular, notice the shift in the field vector orientation at the juncture of the shunt and the pole piece between 0.15 T and the higher fields.

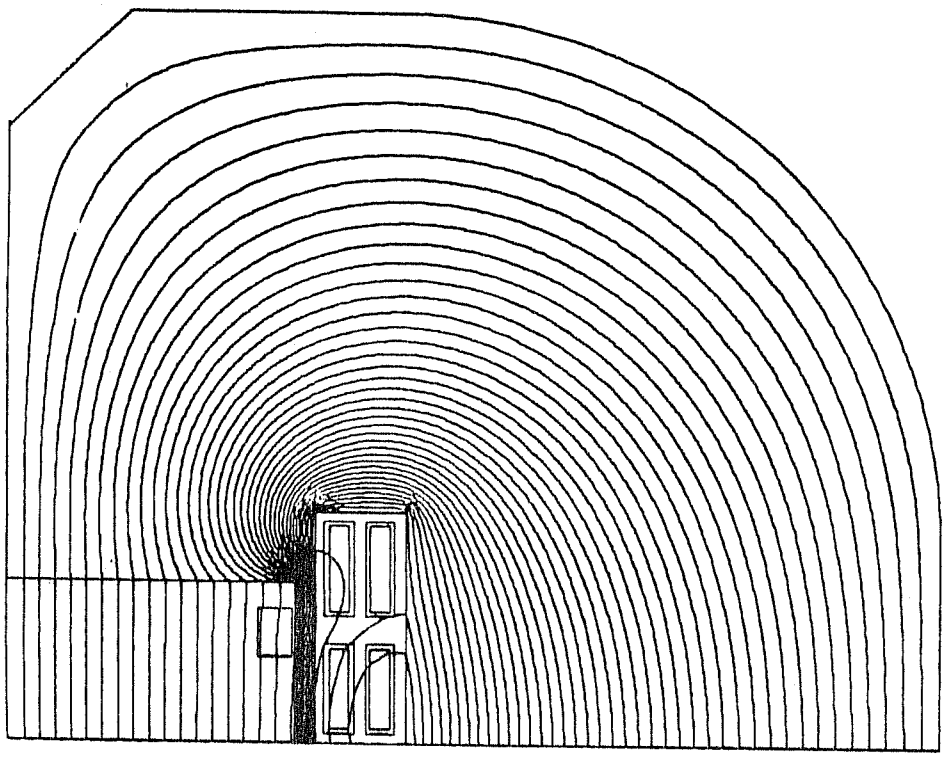

Fig 6, 0.15 T

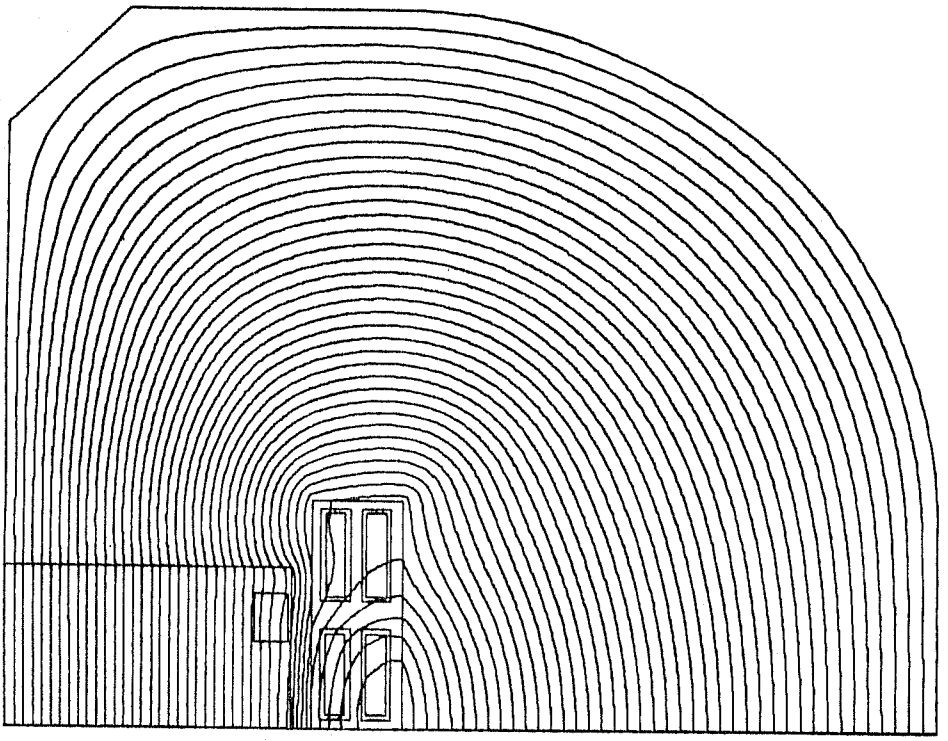

Fig 7, 2.0 T

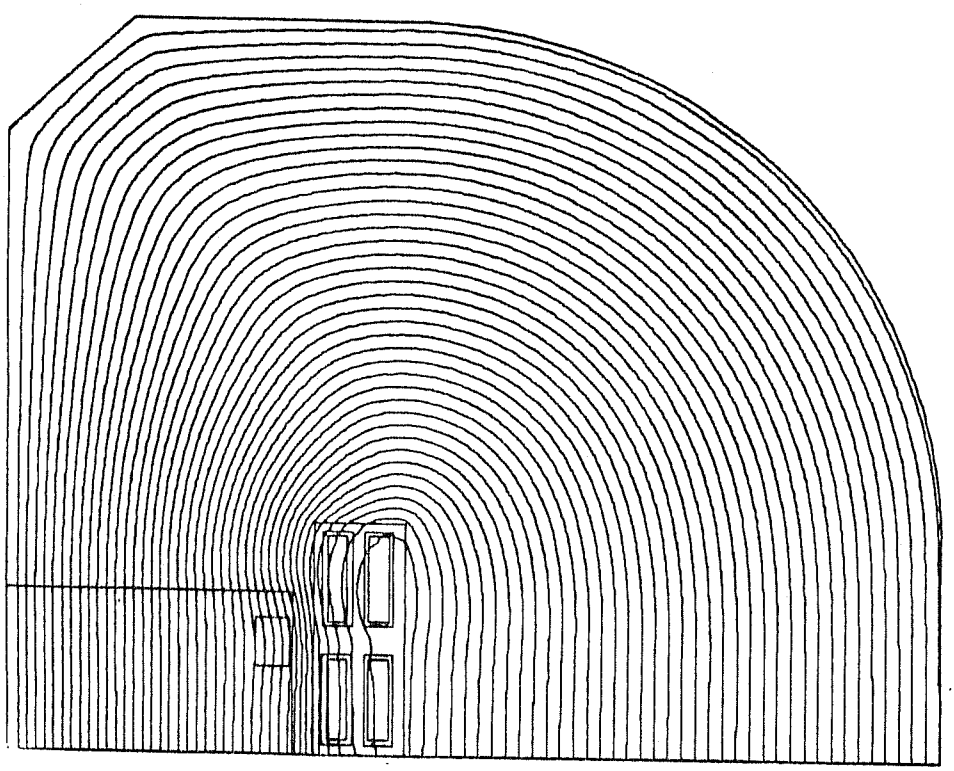

Fig 8, 3.25 T

The shift in field vector orientation in the critical region near the aperture as a function of central field value indicates that the H and B vectors will not remain parallel in this region as the central field value changes. There are several implications related to this magnetization affect. First of all, since H and B are not parallel, the material is magnetically anisotropic and historitic in this region. This presents a difficulty for analysis since computer analysis codes such as POISSON typically treat a material as isotropic, and codes such as PANDIRA, related to POISSON with the additional capability of treating anisotropic permanent magnet materials, do not deal with hysteresis. This situation makes it difficult to predict the significance of the effect numerically.

The hysteresis introduced into the design is again directly related to the presence of the shunt. This is the result of the large difference in flux through the shunt compared to the pole at low fields. At higher fields, due to drop in μ, the differential flux between the shunt and pole piece is small.

The hysteresis will result in a magnet whose tuning characteristics are closely associated with the state of the shunt-pole interface. In particular, a gap or misplacement of the shunt will likely change the tuning characteristics. Since these types of design variations will be different for each magnet, tuning a group of magnets as a whole may present problems.

Part IV - Sensitivity to Up-Down Asymmetries

The asymmetries considered here include material property variations between the top and bottom laminations, and geometric asymmetries of the magnetic shunt. The former category includes a 1% variation in μ and a 1% variation in stacking factor between the top and bottom pole laminations. The latter category includes a .0025 cm gap between the magnetic shunt and the top lamination, and a taper in the magnetic shunt, where the width at the top of the shunt is 99% of the bottom width.

Fig. 9 illustrates the features of the model used for the analysis of these cases. The upper right-hand and lower right-hand quadrants are included to allow for up-down asymmetries. Left-right symmetry is maintained. The details of coil geometry have been simplified in this model compared to the single quadrant model shown in Fig. 1. The location of the trim coil corresponds to the alternated location of Fig. 1.

Again the results reported below refer to the following representation of B^*:

$$B^* = B_x - iB_y = \Sigma\, c_n\, z^n; \quad c_n = a_n + ib_n.$$

For the case of left-right symmetry without up-down symmetry, the allowed coefficients are a_1, a_3, a_5, etc., and b_0, b_2, b_4, etc.

Variations in Pole Laminations

Tables 6, 7 , and 8 report the results for 1% variations in μ and stacking factors between the top and bottom pole laminations; each affect was considered separately. In each case the properties of the top lamination and the magnetic shunt correspond to nominal properties

as used for the single quadrant model. The μ values are from the standard μ table of POISSON; the stacking factor is 100%. The variations in the bottom lamination correspond to the standard μ table multiplied uniformly by 0.99, and a 99% stacking factor.

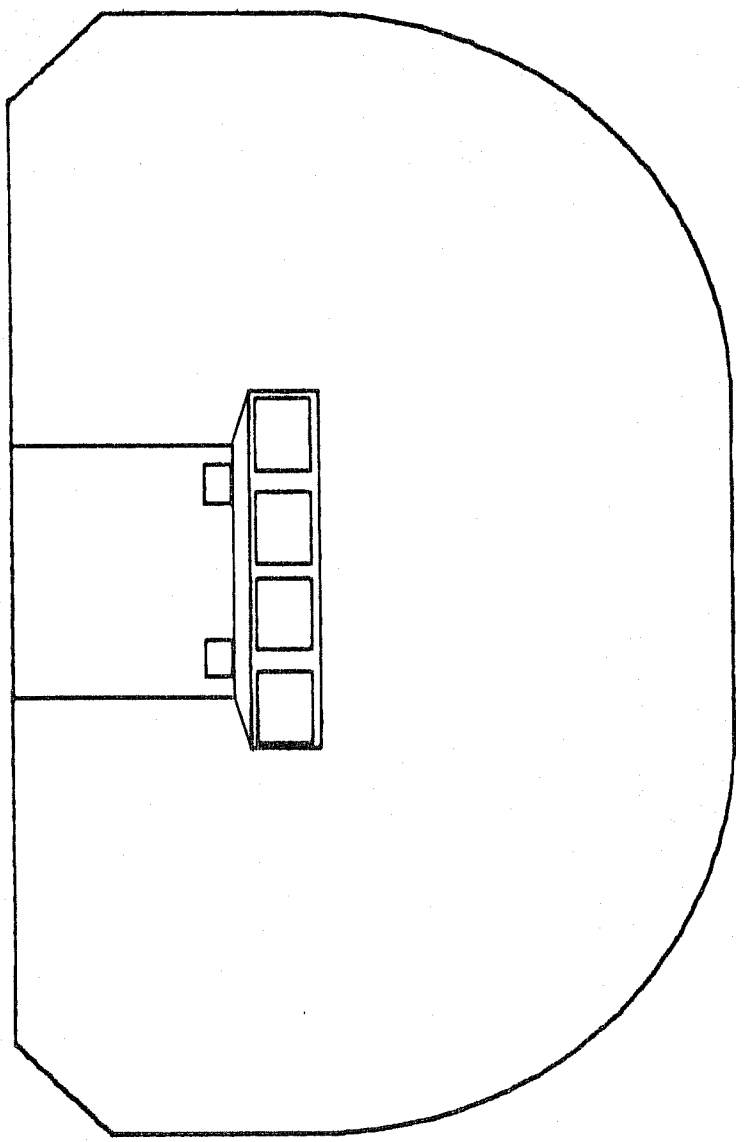

Fig. 9 - Model for Up-Down Symmetry Analysis

Table 6 - 2.0 T

I_c = 2.539 kA, I_{out} = 0.062 kA, I_{in} = 9.258 kA

	Allowed Harmonics				
	Normal Symmetry	δ Stacking Factor		δ μ	
	b_n^1	b_n^2	$\lvert b_n^2\rvert - \lvert b_n^1\rvert$	b_n^3	$\lvert b_n^3\rvert - \lvert b_n^1\rvert$
b_0(T)	2.054	2.052	-0.002	2.054	0.000
$b_2(10^{-4})$	0.643	0.540	-0.103	0.635	-0.008
$b_4(10^{-4})$	3.112	4.493	1.381	3.123	0.015
$b_6(10^{-4})$	0.416	0.477	0.016	0.459	-0.002
$b_8(10^{-4})$	-0.379	-0.383	0.004	-0.383	0.004
$b_{10}(10^{-4})$	0.121	0.123	0.002	0.124	0.003
	Skew Harmonics				
	Normal Symmetry	δ Stacking Factor		δ μ	
	a_n^1	a_n^2	$a_n^2 - a_n^1$	a_n^3	$a_n^3 - a_n^1$
$a_1(10^{-4})$	0.011	-1.077	-1.088	-0.114	-0.125
$a_3(10^{-4})$	-0.068	-0.497	-0.429	-0.100	-0.032
$a_5(10^{-4})$	0.032	0.006	-0.026	0.029	-0.003
$a_7(10^{-4})$	0.094	0.098	0.004	0.093	-0.001
$a_9(10^{-4})$	-0.121	-0.123	-0.002	-0.124	-0.003

Table 7 - 3.0 T

I_c = -2.644 kA, I_{out} = 11.302, I_{in} = 9.957

Allowed Harmonics

	Normal Symmetry b_n^1	δ Stacking Factor b_n^2	$\|b_n^2\| - \|b_n^1\|$	δ μ b_n^3	$\|b_n^3\| - \|b_n^1\|$
b_0(T)	2.939	2.931	-0.008	2.938	-0.001
$b_2(10^{-4})$	13.316	11.804	-1.512	13.069	-0.247
$b_4(10^{-4})$	-2.628	-2.419	-0.209	-2.580	-0.048
$b_6(10^{-4})$	3.365	3.385	0.020	3.373	0.008
$b_8(10^{-4})$	0.579	0.577	-0.002	0.580	0.001
$b_{10}(10^{-4})$	-0.029	-0.035	0.006	-0.034	0.005

Skew Harmonics

	Normal Symmetry a_n^1	δ Stacking Factor a_n^2	$a_n^2 - a_n^1$	δ μ a_n^3	$a_n^3 - a_n^1$
$a_1(10^{-4})$	-0.016	-10.519	-10.503	-2.107	-2.091
$a_3(10^{-4})$	-0.070	-0.800	-0.730	-0.251	-0.181
$a_5(10^{-4})$	0.033	0.048	-0.015	0.029	-0.004
$a_7(10^{-4})$	0.094	0.102	0.008	0.097	0.003
$a_9(10^{-4})$	-0.123	-0.124	-0.001	-0.122	0.001

Table 8 - 3.25 T

I_c = -5.094, I_{out} = 15.278, I_{in} = 11.589

Allowed Harmonics

	Normal Symmetry b_n^1	δ Stacking Factor b_n^2	$\lvert b_n^2\rvert - \lvert b_n^1\rvert$	δ μ b_n^3	$\lvert b_n^3\rvert - \lvert b_n^1\rvert$
b_0(T)	3.213	3.202	-0.104	3.211	-0.082
$b_2(10^{-4})$	-16.584	-15.127	-1.457	-16.478	-0.104
$b_4(10^{-4})$	-5.433	-5.235	-0.198	-5.287	-0.146
$b_6(10^{-4})$	4.066	4.099	0.033	4.044	-0.022
$b_8(10^{-4})$	0.893	0.903	0.010	0.910	0.017
$b_{10}(10^{-4})$	-0.012	-0.012	0.000	-0.009	-0.003

Skew Harmonics

	Normal Symmetry a_n^1	δ Stacking Factor a_n^2	$a_n^2 - a_n^1$	δ μ a_n^3	$a_n^3 - a_n^1$
$a_1(10^{-4})$	-0.010	-12.936	-12.946	-2.590	-2.600
$a_3(10^{-4})$	-0.066	-0.906	-0.840	-0.316	-0.250
$a_5(10^{-4})$	0.033	-0.015	-0.048	0.038	0.005
$a_7(10^{-4})$	0.096	0.119	0.023	0.094	-0.002
$a_9(10^{-4})$	-0.126	-0.132	-0.006	-0.126	0.000

There are several points to note about these results. First of all, the currents for the 3.0 T and 3.25 T cases are not optimized for this coil configuration. Therefore the values for b_2 and b_4 are abnormally high. For this reason the noted change in these values due to the asymmetries is not relevant. The values of primary significance due to up-down asymmetries are the skew terms, the allowed harmonics are however reported for completeness. Note that for the normal symmetry cases, the skew terms, a_1, a_3, etc., should ideally be 0.0. The calculation of these values is a measure of the accuracy of the code in calculating harmonic coefficients.

The most significant result is the value of a_1. In particular, note that the field quality at 3.0 T and 3.25 T is extremely sensitive to variations in stacking factor.

Other Variations in Symmetry

The analysis of the sensitivity to other asymmetries is still in progress. Results have been completed for a 0.0025 cm gap between the top lamination and the shunt, and a 1% taper of the shunt (the top width of the shunt is 99% of the bottom width). The only significant sensitivity (changes in coefficients larger than a unit) that results from these variations is for the case of the tapered shunt at 0.15 T. In this case, $a_1 = -5.7$ units, and $a_3 = -1.4$ units.

Summary and Conclusion

The anlaysis of the magnet as built to specification indicates that with proper current settings the values of b_2 and b_4 can be reduced to acceptable numbers, with the possible exception of intermediate field values around 2.0 T. The results from MIRT suggest some difficulty in tuning for this range of field values. The tunability in this range is however improved by the alternate trim coil location.

Even though b_2 and b_4 are effectively controlled in this design, b_6 becomes large for field values exceeding 3.0 T. At 3.25 T b_6 = 4.756 units.

The field values at the coils become large at high values of the central field. For 3.25 T, the maximum coil field value is 121% of central field. The maximum field point lies on the coil with the highest current. The maximum field value is reduced only slightly by the presence of the shunt. Without the shunt the maximum value increases to 126% of central field.

The magnetic shunt presents a critical boundary condition to the field within the aperture. Field quality at the injection field level is very sensitive to both symmetric and asymmetric geometric and material property perturbations of the shunt.

Asymmetric variations on the order of 1% in either the stacking factor or permeability in the pole laminations result in significant skew quadrupole terms, a_1.